AC transport in granular metals

Author: Carlos Pérez Espinar

Facultat de Física, Universitat de Barcelona, Diagonal 645, 08028 Barcelona, Spain.

Advisor: Dr. Amílcar Labarta Rodríguez

Abstract: AC properties of granular metals nowadays constitute a field of both theoretical and experimental research. In this TFG, we analyze the ac response of granular Co-ZrO$_2$, whose ac electron transport is characterised by randomly competing capacitive conductance and thermally assisted tunneling. Besides, we show that the conductivity, as a function of the frequency, follows a power law which is characteristic of most disordered dielectric materials. The random RC network model will be our tool to discuss WinSpice simulations and drawing conclusions.

I. INTRODUCTION

Granular metal thin films are a unique type of electro-optical device made up of nanoferromagnetic particles randomly embedded in an insulating matrix. Their principal characteristic is the abrupt contrast in electron transport properties depending on the concentration c_0 of metallic nanoparticles within the dielectric medium. These materials exhibit exceptional properties and have a wide range of applications [1]: high-coercive films for information storage, systems where the impedance Z varies non-linearly, screening of electromagnetic waves, etc.
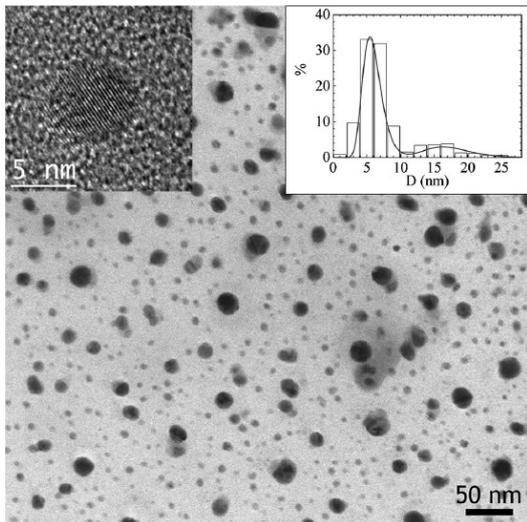

FIG. 1: Example of a real high-resolution transmission electron microscopy (HRTEM) micrograph of granular Co$_{20}$(ZrO$_2$)$_{80}$ [1]. This image also justifies why Co particles can be approximated by spheres.

Generally, the preferred methods for preparing granular metal samples in the laboratory, like the one in Fig.(1), is co-sputtering and laser ablation. These films usually are a few nanometers thick and present an inherent bimodal distribution of nanoparticle radii. Transport properties are mainly due to two mechanisms: temperature dependent quantum tunneling of electrons and capacity conductance between charged surfaces of the em-

bedded metallic particles. Regarding the volume occupied by the metallic fraction c_0, we can clearly distinguish three regimes:

- Metallic regime: $c_0 > c^*$

- Percolation threshold: $c_0 \simeq c^*$

- Dielectric regime: $c_0 < c^*$

where c^* is the concentration above which a tunneling backbone connecting electrode V_+ and V_- appears.

In this paper, we use the random resistor-capacitor (RC) network model in combination with WinSpice software to report on the ac response of a Co-ZrO$_2$ thin film in the regime of low concentrations (dielectric regime), which yields a configuration where the tunneling process is comparable to electrical conduction through capacitance between particles. In order to do so, we will study the disordered nature of electrical paths by analyzing the phase, impedance, electrical modulus and conductivity when the sample is connected to an independent current source.

II. RANDOM RC NETWORK MODEL

The ac properties of a granular metal thin film can be successfully reproduced by a random RC network. Previous studies [2], that focus on the particular case of granular insulating Co-ZrO$_2$ samples, have applied this model by choosing a simplified version of the network: a cubic lattice in which each site is linked with its six nearest neighbours (except for the nodes at the edges and corners) by randomly distributed resistors and capacitors. In general, a fraction $x_r \sim 20\%$ of the electrical bonds is occupied by an "interparticle impedance" of the form $R'_t + i\left(1/C'_p\omega\right)$ where R'_t represents the tunneling resistance and C'_p the capacitive path between smaller particles which are close together, while the remaining bonds $(1 - x_r)$ are occupied by "interparticle capacitive reactances" of the form $i\left(1/C_p\omega\right)$ where C_p represents the capacitive path through larger particles that are further apart. Not only these studies make use of a "censored" version of the model, but they also assign *ad hoc* values

to the resistors and capacitors just to match the experimental data. However, their quantitative results are accurate enough to determine the microscopic parameters that control the ac response of the sample.

Despite of working with such an "oversimplified" and "sketchy" input, the random RC network model is able to recreate the phenomenology of these materials. It is indeed a powerful tool, yet the cubic lattice approach described in the previous paragraph is barely a "first draft" of how the ac current flows through a granular metal thin film. Is for that reason we thought it could be interesting to see what happens when a more realistic RC network is simulated. In particular, a network which brings out the disordering effect of the granular Co arrangement. For that purpose, we have designed a 2D system that mimics the geometric properties of Co-ZrO$_2$ thin films: a bimodal distribution of sizes and randomly scattered Co particles following the Abeles hypothesis of uniform composition in granular media. [3]
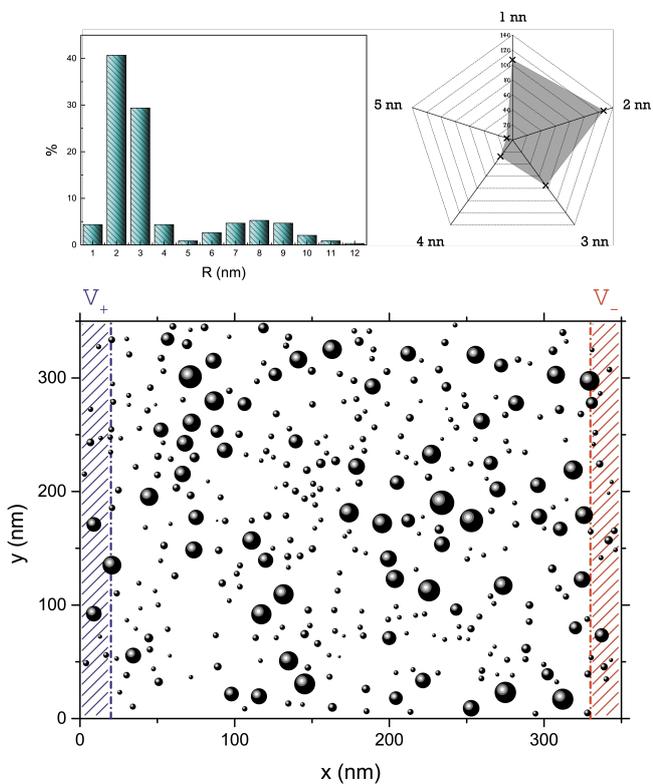

FIG. 2: The normalized histogram exhibits a superposition of two lognormal distributions: 83% small and 17% big metallic particles. The radar chart shows the number of neighbours that a particle has at a distance of 5 nm from centre to centre. The last picture is an artistic illustration of the system, with a concentration of $c_0 = 20\%$ and a total of $N = 344$ spheres (particles).

In Fig.(2), black spots symbolize metallic particles as well as nodes of the subsequent circuit to be simulated and the coloured areas V_+ and V_- depict the left and right electrodes, respectively. Connections between

nodes are more "realistic" in the sense that each particle, except for those within the electrodes, is linked with the rest through capacitors ranging from 10^{-18} F to 10^{-20} F. These values are the mutual capacitances of the N spherical conductors [4] embedded in the ZrO$_2$ insulating matrix and have been calculated (see the Appendix) supposing zirconia is structured as a homogeneous dielectric medium with a relative permitivity of $\varepsilon_r = 23$. On the other hand, the tunneling resistance between two particles is computed among nearest neighbours with the inverse quantum of the tunneling probability formula multiplied by a scale factor:

$$R_t = R_0 e^{2\alpha d_s} \tag{1}$$

where $\alpha = \sqrt{2m_e(V_0 - E)}/\hbar$ is constant for all particles and d_s is the distance between the surfaces of two particles. Notice that varying the height of the potential barrier, typically $\sim$ eV, is an effective way of changing the temperature of the system. [5]

III. RESULTS AND DISCUSSION

Simulations were carried out using WinSpice software and adjusting conveniently the R_0 and α parameters of the system described in Fig.(2). For a more convenient analysis of these two values, Eq.(1) was rewritten into a more compact expression:

$$R_t = R_0 e^{d_s/d_0} \tag{2}$$

where now the microscopic parameters of the exponential function are aggregated to d_0. After performing an ac analysis for various R_0 and d_0 values, the most illustrative cases which will be discussed are: $R_0 = 10^{12}, 10^{13}, 10^{14}$ Ω and $d_0 = 1, 5, 10$ nm. Another important aspect to mention is the meaning of computing R_t "among nearest neighbours" taking into account that Fig.(2) is not a regular array, for example a cubic lattice. It is crucial to state clearly this definition in view of the fineness of the exponential term, which diverges when d_s is large, since adding too much resistors to the circuit could overload WinSpice and make it work more than necessary. We will say that two particles are neighbours if the centre of the second particle is contained in a sphere of radius $5d_0$ centered at the origin of the first one or vice versa. By applying the previous definition, it can be proved that the smallest R_t differs two orders of magnitude from the largest one. Likewise, the number of electrical bonds was also computed in each simulation and x_r ranged from 10% to 20% as expected from experimental results. [5]

As already mentioned before, the fraction of dielectric medium occupied by metallic particles is $c_0 = 20\%$, implying that the simulated sample works in the so-called dielectric regime where the absorption phenomenon related to random competing conduction channels between thermally assisted tunneling and capacitive conductance

occurs. Now, having then explained the way to tackle this project, we are in a position to reproduce the ac properties of Co-ZrO$_2$ thin films. It could seem nothing is missing, but there is still a tricky detail which may go overlooked. Thereby, for the sake of completeness, let us do one last check to verify that the height of the potential barrier $(V_0 - E)$ is actually $\sim$ eV. For example, with $d_0 = 5\ nm$:

$$1/d_0 = 2 \cdot \frac{\sqrt{2m_e\,(V_0 - E)}}{\hbar} \rightarrow (V_0 - E) \approx 0.4 \text{ meV}$$

This is not unreasonable. Barriers used in the simulations do have physical meaning insofar as there is one conduction mechanism called electron hopping that has been ignored since it is hard to differentiate from conventional tunneling. This kind of transport is based on the electronic ability of hopping to neighbouring atomic vacancies and thus moving from one location to another. So, from now on, resistors of the random network will represent a mixed combination of the two processes taking place even though only the tunneling phenomenon will be mentioned. Hence, Eq.(2) has turned out to be an effective R_t which sums up the information regarding both mechanisms.

A. Phase

A deeper insight concerning the arrangement of the RC paths can be achieved by examining the phase φ of the voltage drop across the system as a function of the frequency ν. As Fig.(3) shows, $\varphi\,(\nu)$ scales impressively well by simply multiplying ν by the respective R_0. Not only does this happen with $\varphi\,(\nu)$, but also with most of the remaining magnitudes. With that, we conclude that the effect of increasing R_0 is just shifting the curves to the right.

The two maximums appearing in the $d_0 = 1\ nm$ case are intimately related to the bimodality of the particles. This double peak is reduced for $d_0 = 5\ nm$ because the number of nearest neighbours is considerably larger as the tunneling resistance's exponential term, e^{d_s/d_0}, is less suppressed. For that, smaller particles can now be also connected with bigger particles that are further apart and thus making the resistive connections more "homogeneous". This does not happen for $d_0 = 1\ nm$ where the exponential term is much more suppressed, forcing particles to connect through a R_t following the Abeles hypothesis of uniform composition in granular media or, in other words, through resistive paths between particles with roughly the same size.

At higher temperatures (higher d_0) and lower frequencies, electrical conduction is noticeably governed by thermally assisted tunneling. The second graph in Fig.(3) is a clear example of the expected behaviour $\varphi_{\nu \to 0} \approx 0$ when these conditions are met. As ν is increased, there is a drop in φ since the contributions of capacitive paths
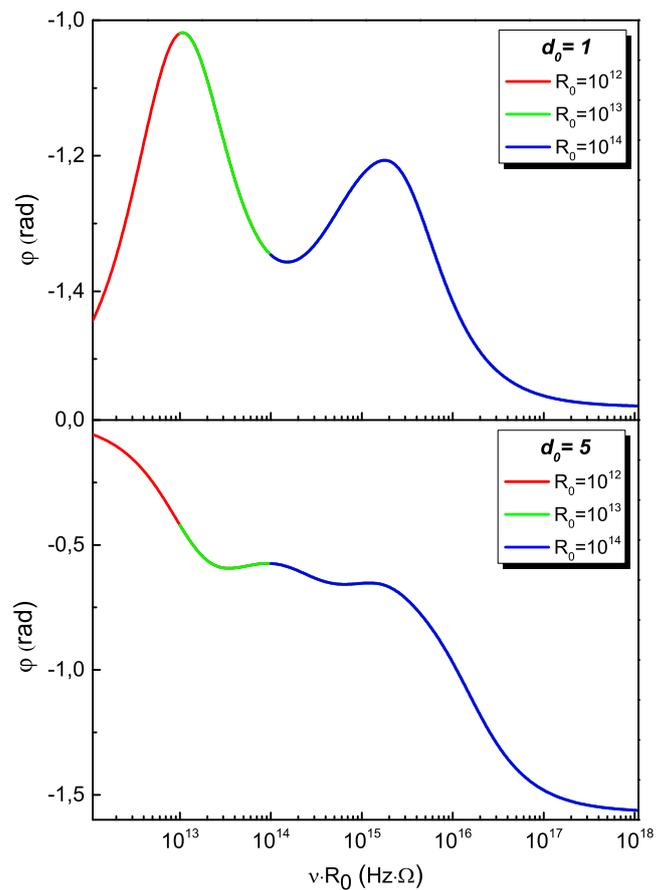

FIG. 3: Phase φ of the RC circuit as a function of the frequency ν for several values of R_0 [Ω] and d_0 [nm]. The corresponding three curves in each figure scale so well that they collapse onto a single master curve.

start to dominate. After that, the constant phase regime (CPR), where $\varphi \approx constant$, is reached. The appearance of a CPR, in the range 10^{13} Hz $\Omega \leq \nu \cdot R_0 \leq 10^{15}$ Hz Ω, is a striking property of granular metals which indicates that the tunneling conduction process is of the same order than the capacitive mechanism. Nonetheless, this phenomenon can be satisfactorily explained by means of capacitive shortcurts appearing along the sample, and hence increasing the electrical conductivity by establishing new bonds with "resistive islands" previously isolated from the tunneling backbone.

B. Impedance and electrical modulus

In order to study the dielectric phenomena undergoing in the granular Co-ZrO$_2$ film, the imaginary part of the impedance $Z''\,(\nu)$, electrical modulus $M''\,(\nu)$ and cole-cole plots provide useful information regarding possible relaxation processes in the system. The real and imaginary parts of the electrical modulus were computed using:

$$M' = \omega C_0 Z'' \qquad (3)$$
$$M'' = \omega C_0 Z' \qquad (4)$$

where $Z = Z' + iZ''$, $M = M' + iM''$, C_0 is the geometrical capacitance $C_0 = \varepsilon_0 A/D$, ε_0 the vacuum permitivity, $A = 7 \cdot 10^3$ nm^2 the electrode area and $D = 310$ nm the distance between electrodes V_+ and V_-. [6]
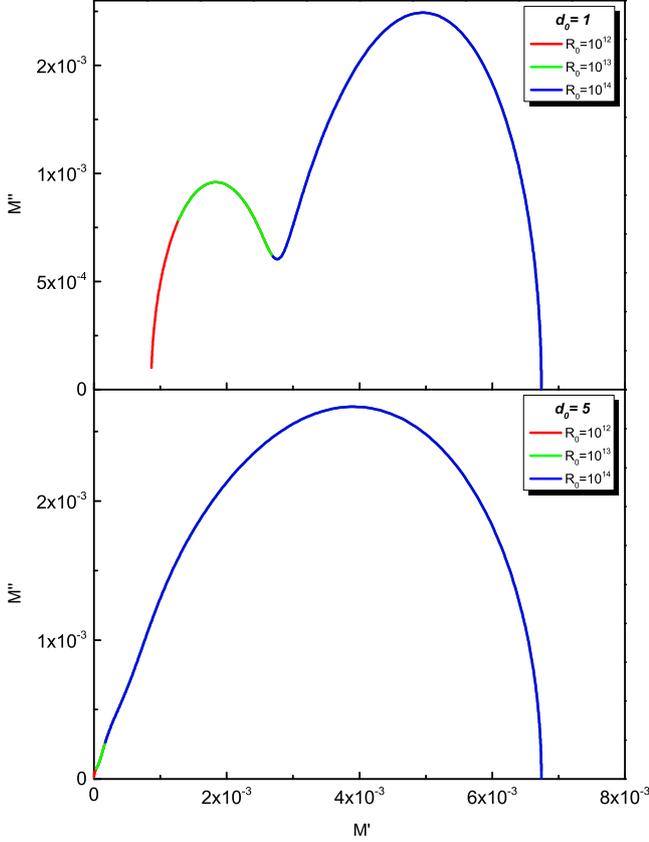
FIG. 4: Cole-cole plots of the electrical modulus for several values of R_0 [Ω] and d_0 [nm].

These Debye-like peaks of Fig.(4) suggest the existence of absorption processes. Particularly, for the $d_0 = 1$ nm case there are two relaxation times associated with it, $\tau_1 = 1/\nu_1^{max}$ (low frequency semicircle) and $\tau_2 = 1/\nu_2^{max}$ (high frequency semicircle) which are again a direct consequence of the bimodality of the particles. The first peak can be explained by the competition of conventional tunneling and capacitive conductance. However, the second peak is due to the same "resistive islands" argument employed in the phase section: large particles are mostly short-circuited and consequently they introduce short-curts along the system, making possible to establish new connections between initially isolated regions at low ν and the tunneling backbone.

Moreover, this complex absorption phenomenon is observed in Fig.(5) too. The discussion made in the previous paragraph can also be applied to interpret the ex-
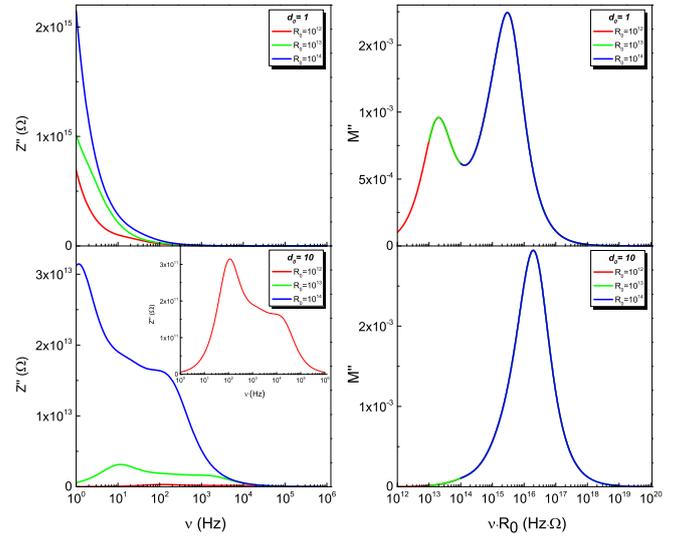
FIG. 5: Imaginary part of the impedance and the electrical modulus as a function of ν for several values of R_0 [Ω] and d_0 [nm]. M'' scales very well but Z'' does not.

istence of multiple peaks in $Z''(\nu)$ and $M''(\nu)$. It is noteworthy that for $d_0 = 1$ nm, $Z'' \to 0$ very quickly but M'' unfolds the richness of Co-ZrO$_2$ thin films' behaviour. Otherwise, for $d_0 = 10$ nm, M'' is not bimodal but Z'' does and, in addition, shows a constant phase regime which can be vaguely appreciated for $R_0 = 10^{12}$ Ω (red curve).

C. Jonscher's UPL model

Granular metals, and many other disordered dielectric materials, display a power law dependence on the real part of the conductivity as a function of the frequency:

$$\sigma'(\omega) = \sigma_{dc} + \beta \omega^n \qquad (5)$$

where σ_{dc} is the conductivity in the dc limit, $\omega = 2\pi\nu$ and β, $0 < n < 1$ are temperature dependent coefficients. This relationship is justified by Jonscher's universal power law (UPL) model, which is in good agreement with experimental and random RC network simulation results. [7]

The overall linear tendency of Fig.(6) proves that Eq.(5) holds for high values of the frequency. The $d_0 = 1$ nm is a case where the effect of having a bimodal distribution of sizes is enhanced, as a consequence, this results in the appearance of two linear trends (instead of just one) connected by a transition regime coloured in green. The fractional exponent n can be easily computed performing a linear regression of the data within the validity range of Jonscher's UPL model (high ν): $n_{d_0=5} \approx 0.88$ and $n_{d_0=1} \approx 0.90$. Additionally, we can use the logarithmic mixing rule [2] to verify that the fractional exponent
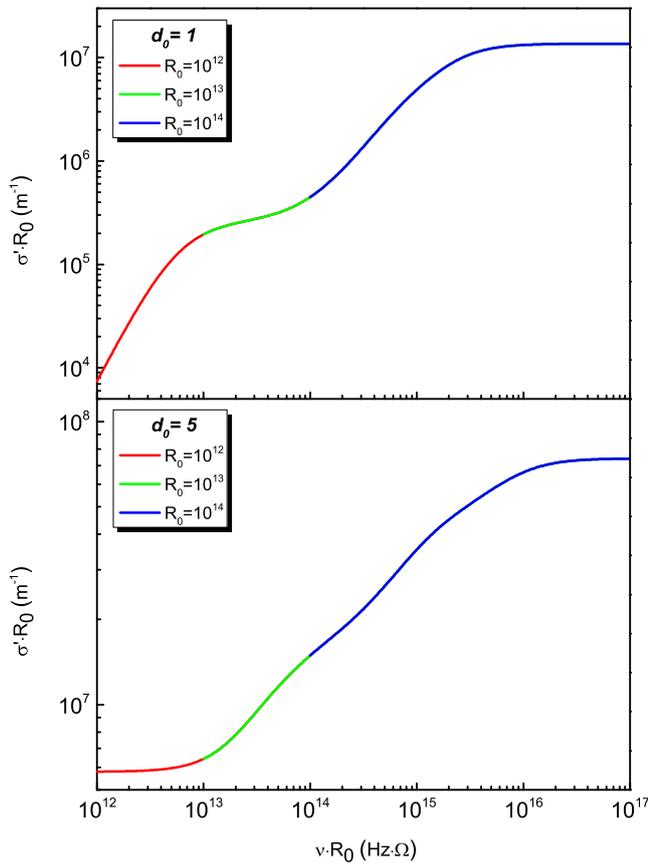
FIG. 6: Log-log graphs of the real part of the conductivity σ' as a function of ν for several values of R_0 [Ω] and d_0 [nm]. In this case, both σ' and ν scale with R_0. The real part of the conductivity was computed using: $\sigma' = (D/A) \cdot \left(Z'/|Z|^2 \right)$, where A is the electrode area and D the distance between electrodes V_+ and V_-.

is bounded between $0 < n < 1$. This phenomenological expression implies that:

$$\sigma(\omega) \approx \left(i\omega\bar{C} \right)^{1-x_r} \qquad (6)$$

where, recall that x_r is the percentage of electrical bonds occupied by resistive paths and $\bar{C}$ is the equivalent capacitance of the network. Note that Eq.(6) establishes a direct relation between n and $1 - x_r$:

$$n = 1 - x_r \longrightarrow x_r \approx 10\% - 20\% \Rightarrow n \approx 0.9 - 0.8$$

IV.   CONCLUSIONS

We have studied the ac response of granular Co-ZrO$_2$ thin films with a Co concentration below the percolation threshold ($c_0 = 20\%$) throughout an improved version of the random RC network model. We conclude that this model successfully reproduces the ac properties of granular metals, especially the electron transport mechanisms: a random competition between thermally assisted tunneling and capacitive conductance among Co particles (respectively represented by resistors and capacitors in the RC network). Besides, we show that $\varphi(\nu)$, $M''(\nu)$, $\sigma'(\nu)$ and the cole-cole curves scale well with the R_0 parameter. We also discuss the relaxation processes that the system exhibits and the implications of having a bimodal distribution of nanoparticle radii. Furthermore, $\sigma'(\nu)$ is found to obey a universal power law characteristic of most disordered dielectric materials.

[1] Konstantinovi, Z., Muro, M. G., Batlle, X., Labarta, A., & Varela, M. (2007). *Nanostructural origin of the ac conductance in dielectric granular metals: The case study of Co₂₀(ZrO₂)₈₀*. Applied Physics Letters, 91(5), 052108. doi:10.1063/1.2766858

[2] Bart Jan Hattink, (2003). *Electrical Properties in Thin Films of Granular Co-ZrO₂. The Oxidation State in Tunnel Junctions* (Doctoral dissertation). Universitat de Barcelona.

[3] Abeles, B., Sheng, P., Coutts, M., & Arie, Y. (1975). *Structural and electrical properties of granular metal films*. Advances in Physics, 24(3), 407-461. doi:10.1080/00018737500101431

[4] Wasshuber, Christoph (1997). *About Single-Electron Devices and Circuits* (Doctoral dissertation), Retrieved from: www.iue.tuwien.ac.at/phd/wasshuber/.

[5] Konstantinovi, Z., Muro, M. G., Kovylina, M., Batlle, X., & Labarta, A. (2009). *Ac conductance in granular insulating Co-ZrO₂ thin films: A universal response*. Physical Review B, 79(9). doi:10.1103/physrevb.79.094201

[6] Bakkali, H., Dominguez, M., Batlle, X., & Labarta, A. (2015). *Equivalent circuit modeling of the ac response of Pd-ZrO₂ granular metal thin films using impedance spectroscopy*. Journal of Physics D: Applied Physics, 48(33), 335306. doi:10.1088/0022-3727/48/33/335306

[7] Bakkali, H., Dominguez, M., Batlle, X., & Labarta, A. (2016). *Universality of the electrical transport in granular metals*. Scientific Reports, 6(1). doi:10.1038/srep29676

APPENDIX

A problem whose complexity goes unnoticed throughout this TFG is the computation of the capacitance matrix of an arbitrary arrangement of N spherical conductors in a homogeneous dielectric medium. The core algorithm is based on the method of images and is further discussed in Christoph Wasshuber's PhD thesis.

The program starts by placing an arbitrary single point charge Q_0 on the centre of the first particle and leaves the $N-1$ remaining particles connected to the ground. As a consequence of the electrostatic field created by Q_0, these $N-1$ conductors are no longer at zero equipotential surfaces. Therefore, the main objective in each iteration will be to add compensation charges within the particles in order to keep this configuration unaltered: $V_1 = Q_0/4\pi\varepsilon R_1$ and $V_{\neq 1} = 0$. It is not quite puzzling to get the general idea; every time an image charge Q' is placed in the system, $N-1$ compensation charges will appear to counter his effect and, consequently, these new compensation charges will have to be nullified again with more Q'' and so on. Can you see the vicious circle? Once this exhausting computation is performed, thanks to the V_1 and $V_{\neq 1} = 0$ clever configuration the program uses

$$c_{ij} = 4\pi\varepsilon R_i \cdot \left| \sum_j \frac{Q_j}{Q_0} \right|$$

where R_i is the radius of the ith particle and Q_j the compensation charges within the jth particle, to calculate all matrix elements.

In WinSpice capacitors are always of the c_{ij} form, and hence positive. That means we only need to take into account the absolute value of the mutual capacitances. By iterating up to a certain cut-off, the algorithm is able to determine the corresponding column of the capacitance matrix referred to the Q_0-particle, that is, one of these:

$$\begin{pmatrix} Q_1 \\ Q_2 \\ \vdots \\ Q_N \end{pmatrix} = \begin{pmatrix} \sum_{k=1}^{N} c_{1k} & -c_{12} & \cdots & -c_{1N} \\ -c_{21} & \sum_{k=1}^{N} c_{2k} & \cdots & -c_{2N} \\ \vdots & \vdots & \ddots & \vdots \\ -c_{N1} & -c_{N2} & \cdots & \sum_{k=1}^{N} c_{Nk} \end{pmatrix} \begin{pmatrix} V_1 \\ V_2 \\ \vdots \\ V_N \end{pmatrix}$$

Finally, to accomplish the task of computing the whole matrix, the program loops through the array where all particles are stored to repeat the process described in the second paragraph over all particles. However, the difficult part is to have the algorithm converge. After doing some testing, we conclude that if the spheres are too dense arranged it is impossible to achieve convergence. So, an approximated formula was used to work out the mutual capacitances for the furthest particles,

$$\left| c_{ij}^{approx} \right| = 4\pi\varepsilon \frac{R_i R_j}{d}$$

where d is the interparticle distance between centres, and my implementation applied only among nearest neighbours. It is indeed a crude approximation but the results are of the same order of magnitud that we expected, so... *se non è vero, è ben trovato!*